Power Efficient Wireless Sensor Node through Edge Intelligence

Abhishek Priyadarshan Damle*, Sook Shin Ha*, Zhuqing Zhao*, Barbara Roqueto dos Reis**, Robin White**, and Dong Sam Ha*
*Multifunctional Integrated Circuits and System (MICS) Group
Bradley Department of Electrical and Computer Engineering
**Dept of Animal and Poultry Sciences
Virginia Tech, Blacksburg, Virginia, 24061, USA
E-mail: {adamle, sook, zhuqing8, barbarar, rrwhite, ha} @vt.edu

***Abstract* — Edge intelligence can reduce power dissipation to enable power-hungry long-range wireless applications. This work applies edge intelligence to quantify the reduction in power dissipation. We designed a wireless sensor node with a LoRa radio and implemented a decision tree classifier, in situ, to classify behaviors of cattle. We estimate that employing edge intelligence on our wireless sensor node reduces its average power dissipation by up to a factor of 50, from 20.10 mW to 0.41 mW. We also observe that edge intelligence increases the link budget without significantly affecting average power dissipation.**

Keywords — Edge intelligence, LoRaWAN, smart farm, cattle behavior, decision tree classifier.

I. Introduction

Traditional IoT networks collect data on edge nodes and wirelessly transmit it to central cloud servers for processing. However, transmitting raw data significantly strains wireless networks and cloud servers, as they must deal with vast quantities of data. Edge intelligence reduces the burden by processing data on edge nodes using machine learning [1-3]. This technique is valuable for low-power wide-area networks (LPWANs), which have relatively small bandwidths and data rates. LPWANs can be applied to smart agriculture and livestock raising, where battery-powered end nodes transmit data over several kilometers [4-7]. The radios on LPWAN nodes dissipate significant power since they must transmit data over long ranges. Reducing the amount of wirelessly transmitted data through machine learning would reduce power dissipation.

A specific application of LPWANs is the welfare assessment of livestock. Animal agriculture has intensified over the past several decades, and animals are increasingly managed as large groups, rather than individuals [8]. Group-based management increases animal productivity, but monitoring of individual animals is labor-intensive [9]. Wireless sensor nodes (WSNs), integrated with LPWANs, can continuously monitor individual animals effectively [10-12] to reduce production losses through early detection of diseases [13, 14]. However, the significant energy required for long range data transmission is a major challenge for smart agriculture [15].

This work aims to reduce power dissipation of a WSN through edge intelligence. We designed a WSN to monitor the activities of cattle by sensing acceleration data. The data were processed with a machine learning algorithm on the WSN to classify cattle behaviors. We measured the classification performance of the machine learning model and the power dissipated by our WSN while collecting, processing, and transmitting data.

This paper is organized as follows. Section II provides background on LoRa and a decision tree classifier. Section III overviews the proposed WSN and processing of machine learning algorithm on the WSN. Section IV presents and discusses the results, while Section V concludes the paper.

II. Background

A. LoRa and LoRaWAN

LoRa uses chirps as carrier signals, whose frequency oscillates between a minimum and maximum value [16]. The spreading factor determines the speed of a chirp. LoRa wide area network (LoRaWAN) uses LoRa modulation to create LPWANs in a star topology comprising end nodes, gateways, network servers, and application servers. It adds a minimum of 13 bytes to each payload transmitted from an end node to the gateways [17]. LoRa's bit rate, range, and time on air rely on the spreading factor. Chirps are faster for lower spreading factors, which increase the bit rates and reduce the time on-air. The reduced time on-air decreases the power dissipation during data transmission [18]. However, a lower spreading factor has a lower processing gain, which decreases the transmission range [18]. Therefore, the trade-off between power dissipation and range needs to be balanced when selecting the appropriate spreading factor.

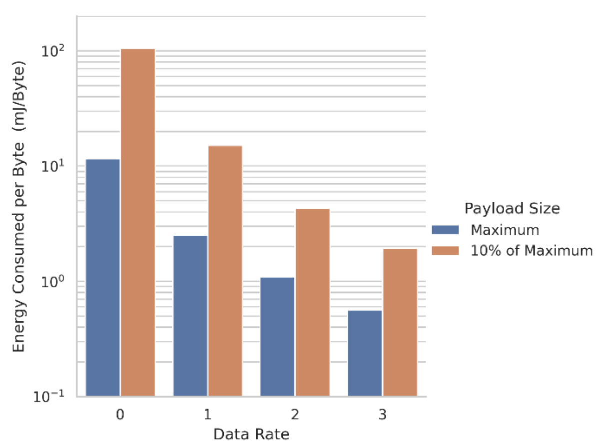

Fig. 1. Energy per byte of data transmitted as a maximum and fractional payload at varying data rates.

The time on-air has several constraints. The biggest one is the energy required for data transmission. Additionally, there are country-specific caps on dwell time [19]. Network servers also impose similar restrictions on time on-air to ensure that LoRaWAN can serve many devices [20]. The restriction on time on-air limits the payload size for the various spreading factors. Due to the overhead of the LoRaWAN protocol, far less energy per byte is used to transmit a maximum payload than its fractional portion, as shown in Fig. 1. Table I shows the relationship between spreading factor, bit rate, range, receiver sensitivity, and maximum payload size [18, 21].

TABLE I. Relationship between the data rate, spreading factor, bit rate, maximum payload, receiver sensitivity, and range [18, 21].

Data Rate	Spreading Factor	Bit rate (bits/s)	Maximum Payload (B)	Receiver Sensitivity (dBm)	Range (km)
0	10	980	11	-132	8
1	9	1,760	53	-129	6
2	8	3,125	125	-126	4
3	7	5,470	242	-123	2

B. Decision Tree Classifier

A decision tree classifier is a supervised machine learning algorithm used for regression and classification [22, 23]. It starts at the root node and sorts data based on criteria determined by the decision nodes, until it reaches a terminal node. The criteria used by the decision nodes are selected as part of the training process, which attempts to divide the dataset into increasingly homogeneous subsets. Decision trees have a distinct advantage because they can be efficiently implemented. The decision nodes are implemented through conditional statements. Thus, a series of conditional statements creates a decision tree classifier. Compilers recognize and optimize these conditional statements in efficient forms, such as jump tables.

III. Proposed WSN and Implementation of Machine Learning

A. Wireless Sensor Node (WSN)

The proposed WSN collects 3-axis acceleration data from cattle and transmits it through LoRa. It consists of a Bosch BMA 400 ultra-low power 3-axis accelerometer [24] to collect motion data, and a Microchip WLR089U0 module [25] to process and transmit it. Fig. 2(a) shows a high-level block diagram of the WSN. The WLR089U0 module combines an ATSAMR34J18B SiP and external components. The SiP contains an ARM Cortex M0+ processor with 256 KiB of flash storage, 32 KiB of SRAM, and 8 KiB of low-power SRAM. It also contains a LoRa transceiver with 863 MHz to 928 MHz dual-band coverage, and maximum transmission power of 18.59 dBm.

A 12-bit accelerometer with the range of ± 2g samples acceleration on the x-, y-, and z- axes with a sample rate of 50 Hz. It uses a low-pass filter with a cutoff frequency of 24 Hz to reduce aliasing and a 1 KiB FIFO buffer to store up to 146 readings. Once the FIFO becomes full, the data are transferred to the micro-controller unit (MCU) for processing. We prototyped the WSN with a custom PCB, as shown in Fig. 2(b), with dimensions 54 mm × 38 mm.

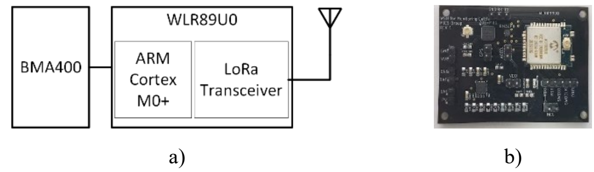

Fig. 2. a) Block diagram of the WSN b) prototype.

Fig. 3 shows the flowchart of the MCU operation. The primary activities of the MCU are data collection and processing, data transmission, and sleeping, while feature extraction and classification are minor in terms of the processing time.

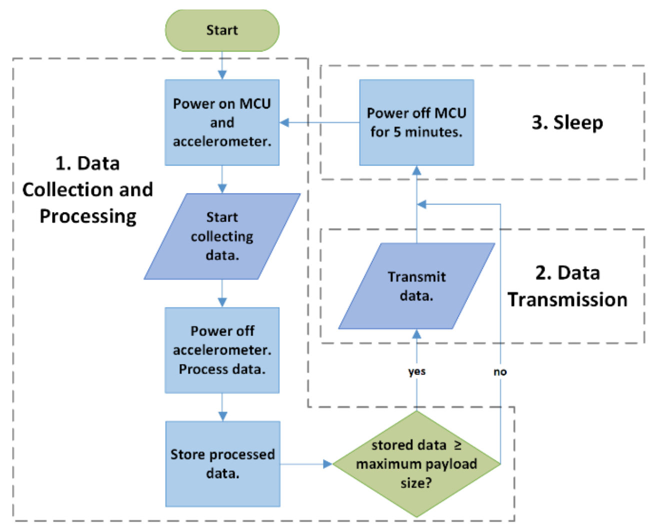

Fig. 3. Flowchart of the WSN's operation.

B. Dataset, Feature Extraction, and Feature Selection

We mounted WSNs on the halters of five different cows and recorded their activities. After cleaning and labeling the collected data, the dataset consists of 31 hours in total for five activities including grazing (11.86 h), ruminating (8.86 h), lying (6.44 h), standing (2.95 h), and walking (0.89 h).

We extracted time and frequency domain features from the dataset. All features were calculated using a C program to ensure the feature extraction is identical during training and on the MCU. The frequency domain features were calculated with help of the KISS FFT library [26]. We calculated the features as 32-bit signed integers and standardized them such that the mean was $2^{16}/2$, while the standard deviation was $2^{16}/4$. Data greater than or less than two standard deviations were clipped to 0 and 2^{16}-1, respectively. Resultantly, the standardized features were stored as 16-bit unsigned integers with the range of [0, 2^{16}-1]. We selected the ten best features using recursive feature elimination (RFE) to train our decision tree model and avoid saturation of the classification performance. These features are the sum of absolute values of x-axis, sum of absolute values of y-axis, median of x-axis, median of y-axis, average intensity, entropy of x-axis, entropy of z-axis, peak spectral density (PSD) between 0-8 Hz of y-axis, PSD between 8-25 Hz of y-axis, and PSD between 8-25 Hz of z-axis.

C. *Implementation of Machine Learning on MCU*

We used cost complexity pruning [27] to limit the complexity of our decision trees and avoid overfitting training data. Through tenfold cross-validation, we determined pruning trees using a pruning parameter of 1.062×10^{-4}, resulted in 353 nodes and the best classification performance. We trained the decision tree model using the scikit-learn library [28] in python and ported it to C using the emlearn library [29]. The decision tree model in C was paired with the feature extraction and standardization programs to classify cattle behaviors using raw accelerometer data as the input. Fig. 4 outlines the three processing stages to classify cattle behaviors based on accelerometer data. The first stage decodes 1 KiB of encoded accelerometer data to 876 B. The next stage performs feature extraction on the decoded accelerometer data and outputs 20 B of features. The final stage uses the features as inputs for a decision tree model and outputs a behavior stored as 1 B.

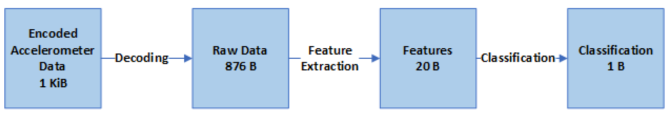

Fig. 4. Pipeline to process the accelerometer data.

IV. Measurement Results and Discussion

A. *Classification Performance*

We evaluated the performance of our decision tree model using tenfold cross-validation. Fig. 5 shows the overall confusion matrix of the model. The head posture of cattle during lying and standing is similar, causing the decision tree to confuse the two behaviors. The cattle also tend to walk slowly while grazing, leading to confusion between walking and grazing activities. Table II shows the classification report. Our model classifies grazing, lying, and ruminating behaviors well, while standing and walking behaviors have the lowest F1-scores. Our model has higher F1-scores than a support vector classifier [30] and comparable performance to a decision tree classifier [31] and multilayer perceptron classifier [32].

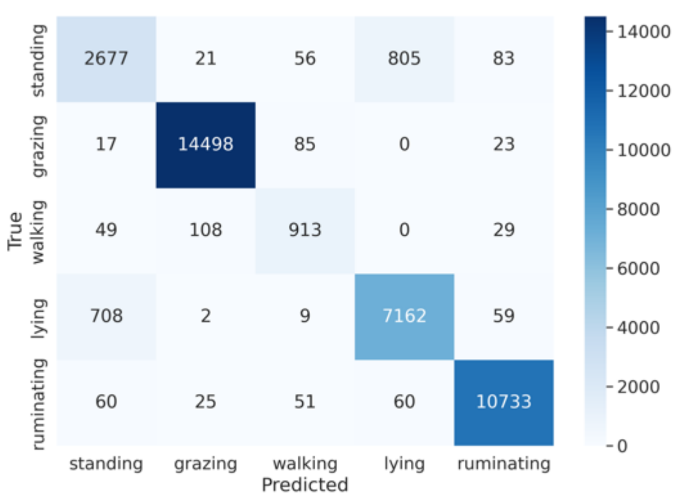

Fig. 5. Confusion matrix of the decision tree model.

TABLE II. Classification Report of the Decision Tree Model

	Precision	Recall	F1-Score	Support
Standing	0.7625	0.7350	0.7485	3642
Grazing	0.9894	0.9915	0.9904	14623
Walking	0.8196	0.8308	0.8251	1099
Lying	0.8922	0.9020	0.8971	7940
Ruminating	0.9822	0.9821	0.9822	10929
Accuracy	0.9412			

B. *Power Dissipation*

We measured the power dissipation of the WSN using an INA280 current amplifier and a shunt resistor. Fig. 6 shows the instantaneous power dissipation of the WSN. The power dissipated while collecting and processing accelerometer data is shown in Fig. 6(a), while Fig. 6(b) shows the power dissipated during data transmission, and Fig. 6(c) shows the power dissipated when the WSN is asleep. All three activities are shown in Fig. 6(d) and correspond to the labeled sections of the flowchart in Fig. 3. The WSN's peak power dissipation is 276.40 mW during data transmission whereas all other activities dissipate less than 5 mW.

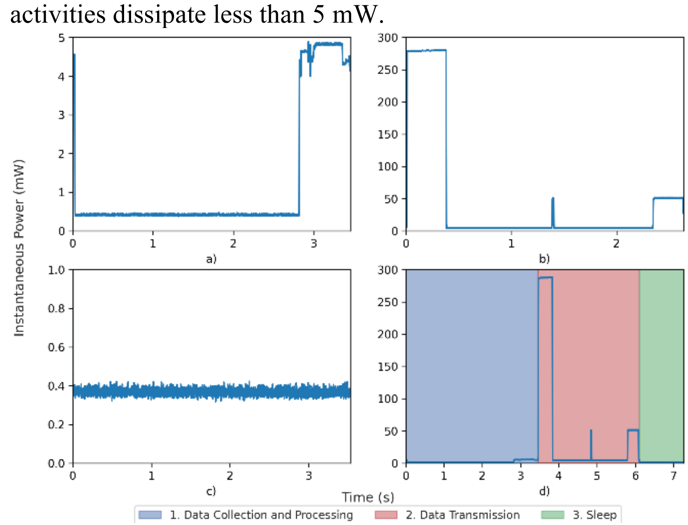

Fig. 6. Instantaneous power dissipation a) for data collection and processing b) for data transmission c) during sleep d) total power dissipation of the WSN.

The energy consumed by each major activity of the WSN is displayed in Fig. 7. Data collection and processing is divided into the baseline, feature extraction, and classification stages. The baseline stage consists of collecting and decoding accelerometer data. The decoded accelerometer data is then processed further in the feature extraction and classification stages as shown in Fig. 4. Data transmission consumes 133.32 mJ, by far the most energy on the WSN. The WSN also consumes 108.36 mJ during its sleep period, primarily because this period lasts for five minutes, whereas the other tasks only last for several seconds. Compared to the energy used during data transmission, the baseline, feature extraction, and classification tasks consume only a total of 4.23 mJ of energy. Thus, the key to reducing the average power dissipation of the WSN is to limit the wirelessly transmitted data by processing it in situ.

Fig. 8(a) shows the energy used to transmit a batch of data processed to varying degrees. The baseline level of processing represents the decoding stage shown in Fig. 4. Feature extraction reduces the size of a batch of data to 20 B, while classification reduces it further to only 1 B. Through feature extraction and classification, more batches of data can be transmitted in a single payload, reducing the energy used to transmit the batch of data. Per Table 1, as LoRaWAN's data rate increases from 0 to 3, the maximum payload size increases from 11 B to 242 B. Thus, payloads transmitted at higher data rates can store more batches of data per payload. This also leads to a decrease in the energy used to transmit a batch of data.

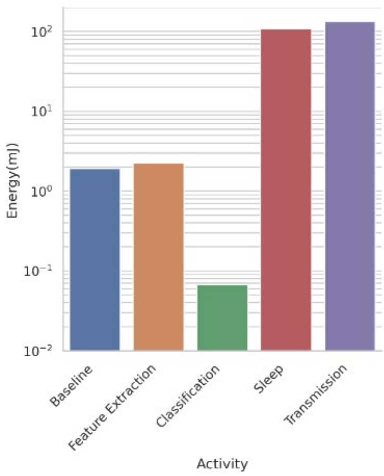

Fig. 7. Energy consumed by the WSN performing various activities.

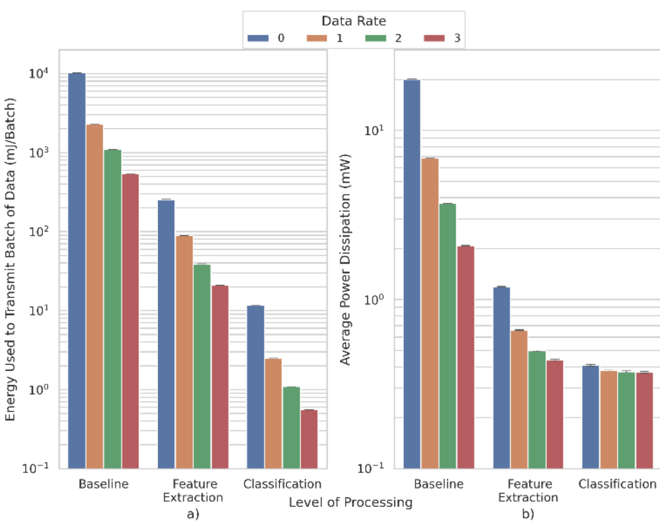

Fig. 8. a) Energy used to transmit a batch of data processed to varying degrees. b) average power dissipation of the WSN

Using the logic from Fig. 3, we estimated the average power dissipation of the WSN while it processed data to varying degrees and transmitted it at various data rates. Fig. 8(b) shows the average power dissipated by our WSN under these conditions. The power dissipation of the WSN increases as the data rate decreases. This is because smaller data rates support smaller payloads. Therefore, the WSN can accumulate fewer batches of data in a payload and transmits more frequently. However, if only classification results are transmitted, the average power dissipation of the WSN is not significantly affected by the data rate of transmission. For transmitting data using data rates 0 and 3, we only observe a difference of 36.09 μW. This is because data are transmitted infrequently compared to if the features or raw data are transmitted. For instance, the WSN transmits raw data every 2.96 s (for all data rates), features between 3.43 s (for data rate 0) and 3644.67 s (for data rate 3), and classifications between 3037.95 s (for data rate 0) and 73134.92 s (for data rate 3). Due to infrequent transmissions, the power dissipation of the other processes dominates the average power dissipation, and the data rate does not significantly impact it. Since lower data rates have greater processing gain, the link budget of our WSNs can be increased by using data rate 0 without significantly increasing power dissipation. This allows other aspects, such as transmission range, transmission power, and antenna design, to be optimized to best use the additional link budget.

The combination of the decreased energy per batch of data transmitted and the decreased frequency of transmissions, significantly lowers the average power dissipation per data rate and level of processing. The impact of processing data to higher degrees on the average power dissipation of the WSN is most significant when data are transmitted with a data rate of 0 and least when they are transmitted with a data rate of 3. Compared to the baseline, computing and transmitting features results in a maximum power reduction of 18.91 mW (from 20.10 mW to 1.19 mW) and a minimum power reduction of 1.65 mW (from 2.08 mW to 0.44 mW). Meanwhile, computing and transmitting classifications results in a maximum power reduction of 19.69 mW (from 20.10 mW to 0.41 mW) and a minimum power reduction of 1.71 mW (from 2.08 mW to 0.37 mW).

V. Conclusion

This work highlights that edge intelligence significantly reduces power dissipation of WSNs. We quantified the reduction of power dissipation using an example of cattle behavior monitoring and observed that the power dissipated by our WSN was up to 50 times smaller when we applied machine learning in situ instead of transmitting raw data. For LPWANs, we also observed that using edge intelligence confers a consequential advantage, as it increases the link budget without significantly affecting the average power dissipation of the WSN. The increased link budget can be used to increase transmission range, decrease transmission power, or reduce the antenna size of the WSN.

The decrease in power dissipation is achieved through increasing the amount of behavioral data in a transmission and reducing the frequency of transmissions. In the future, the WSN could mitigate the tradeoff between power dissipation and latency by intelligently deciding when to transmit data. The WSN could store statistical models of an individual cow's behaviors based on historic data. A set of newly classified behavior data could then be compared to this model and anomalous trends reported in real time.

Acknowledgment

This research was supported in part by the National Science Foundation Award no. 2106987.

References

[1] S. Deng, H. Zhao, W. Fang, J. Yin, S. Dustdar, and A. Y. Zomaya, "Edge Intelligence: The Confluence of Edge Computing and Artificial Intelligence," *IEEE Internet of Things Journal,* vol. 7, no. 8, pp. 7457-7469, August 2020, doi: 10.1109/jiot.2020.2984887.

[2] Z. Zhou, X. Chen, E. Li, L. Zeng, K. Luo, and J. Zhang, "Edge Intelligence: Paving the Last Mile of Artificial Intelligence With Edge Computing," *Proceedings of the IEEE,* vol. 107, no. 8, pp. 1738-1762, August 2019, doi: 10.1109/jproc.2019.2918951.

[3] S. Liu, D. S. Ha, F. Shen, and Y. Yi, "Efficient neural networks for edge devices," *Computers & Electrical Engineering,* vol. 92, p. 107121, 2021-06-01 2021, doi: 10.1016/j.compeleceng.2021.107121.

[4] M. L. Liya and D. Arjun, "A Survey of LPWAN Technology in Agricultural Field," presented at the 2020 Fourth International Conference on I-SMAC, 2020.

[5] F. Pasandideh, B. Ray, N. Islam, and C. A. A. Ieee International Conference on Smart Internet of Things Beijing, "IoT Based Smart Farming: Are the LPWAN Technologies Suitable for Remote Communication?," presented at the 2020 IEEE International Conference on Smart Internet of Things (SmartIoT), 2020.

[6] G. Valecce, P. Petruzzi, S. Strazzella, and L. A. Grieco, "NB-IoT for Smart Agriculture: Experiments from the Field," in *2020 7th International Conference on Control, Decision and Information Technologies (CoDIT)*, 2020: IEEE, doi: 10.1109/codit49905.2020.9263860.

[7] C. Yoon, M. Huh, S.-G. Kang, J. Park, and C. Lee, "Implement smart farm with IoT technology," in *2018 20th International Conference on Advanced Communication Technology (ICACT)*, 2018: IEEE, doi: 10.23919/icact.2018.8323908.

[8] J. L. Capper, "Replacing rose-tinted spectacles with a high-powered microscope: The historical versus modern carbon footprint of animal agriculture," *Animal Frontiers,* vol. 1, no. 1, pp. 26-32, July 2011, doi: 10.2527/af.2011-0009.

[9] D. M. Liebe and R. R. White, "Analytics in sustainable precision animal nutrition," *Anim Front,* vol. 9, no. 2, pp. 16-24, Apr 2019, doi: 10.1093/af/vfz003.

[10] B. Sharma and D. Koundal, "Cattle health monitoring system using wireless sensor network: a survey from innovation perspective," *IET Wireless Sensor Systems,* vol. 8, no. 4, pp. 143-151, August 2018, doi: 10.1049/iet-wss.2017.0060.

[11] I. Andonovic *et al.*, "Wireless Sensor Networks for Cattle Health Monitoring," in *ICT Innovations 2009*: Springer Berlin Heidelberg, 2010, pp. 21-31.

[12] M. Gameil and T. Gaber, "Wireless Sensor Networks-Based Solutions for Cattle Health Monitoring: A Survey," presented at the International Conference on Advanced Intelligent Systems and Informatics, 2019.

[13] J. D. Reader, M. J. Green, J. Kaler, S. A. Mason, and L. E. Green, "Effect of mobility score on milk yield and activity in dairy cattle," (in English), *J. Dairy Sci.,* Article vol. 94, no. 10, pp. 5045-5052, October 2011, doi: 10.3168/jds.2011-4415.

[14] J. M. Huzzey, D. M. Veira, D. M. Weary, and M. A. G. Von Keyserlingk, "Prepartum Behavior and Dry Matter Intake Identify Dairy Cows at Risk for Metritis," *J. Dairy Sci.,* vol. 90, no. 7, pp. 3220-3233, July 2007, doi: 10.3168/jds.2006-807.

[15] M. R. M. Kassim, "IoT Applications in Smart Agriculture: Issues and Challenges," in *2020 IEEE Conference on Open Systems (ICOS)*, November 2020: IEEE, doi: 10.1109/icos50156.2020.9293672.

[16] L. Vangelista, "Frequency Shift Chirp Modulation: The LoRa Modulation," *IEEE Signal Processing Letters,* vol. 24, no. 12, pp. 1818-1821, December 2017, doi: 10.1109/lsp.2017.2762960.

[17] D. Bankov, E. Khorov, and A. Lyakhov, "On the Limits of LoRaWAN Channel Access," in *2016 International Conference on Engineering and Telecommunication*, 2016: IEEE, doi: 10.1109/ent.2016.011.

[18] Semtech, "LoRa® and LoRaWAN®: A Technical Overview," December 2019. [Online]. Available: https://lora-developers.semtech.com/uploads/documents/files/LoRa_and_LoRaWAN-A_Tech_Overview-Downloadable.pdf

[19] LoRa Alliance Technical Committee Regional Parameters Workgroup, "RP002-1.0.1 LoRaWAN® Regional Parameters," February 20 2020. [Online]. Available: https://lora-alliance.org/wp-content/uploads/2020/11/rp_2-1.0.1.pdf

[20] "Duty Cycle " The Things Network. https://www.thethingsnetwork.org/docs/lorawan/duty-cycle/#fair-use-policy (accessed October 24, 2021).

[21] Semtech Corporation, "AN1200.22 LoRa™ Modulation Basics," AN1200.22, May 2015. [Online]. Available: http://www.semtech.com/images/datasheet/an1200.22.pdf

[22] W. Y. Loh, "Classification and regression trees," *WIREs Data Mining and Knowledge Discovery,* vol. 1, no. 1, pp. 14-23, 2011 2011, doi: 10.1002/widm.8.

[23] S. R. Safavian and D. Landgrebe, "A survey of decision tree classifier methodology," *IEEE Transactions on Systems, Man, and Cybernetics,* vol. 21, no. 3, pp. 660-674, May-June 1991, doi: 10.1109/21.97458.

[24] Bosch Sensortec, "BMA400 - Data Sheet," July 2019. [Online]. Available: https://www.bosch-sensortec.com/media/boschsensortec/downloads/datasheets/bst-bma400-ds000.pdf

[25] "WLR089U0 Low Power LoRa® Sub-GHz Module Data Sheet," Feburary 2021. [Online]. Available: https://ww1.microchip.com/downloads/en/DeviceDoc/70005435B.pdf

[26] M. Borgerding, "KISS FFT," 2003. [Online]. Available: https://github.com/mborgerding/kissfft

[27] F. Esposito, D. Malerba, G. Semeraro, and J. Kay, "A comparative analysis of methods for pruning decision trees," *IEEE Transactions on Pattern Analysis and Machine Intelligence,* vol. 19, no. 5, pp. 476-493, May 1997, doi: 10.1109/34.589207.

[28] F. Pedregosa *et al.*, "Scikit-learn: Machine Learning in Python," *Journal of Machine Learning Research,* vol. 12, pp. 2825-2830, 2011.

[29] J. Nordby, "emlearn: Machine Learning inference engine for Microcontrollers and Embedded Devices," March 2019, doi: 10.5281/zenodo.2589394.

[30] P. Martiskainen, M. Järvinen, J.-P. Skön, J. Tiirikainen, M. Kolehmainen, and J. Mononen, "Cow behaviour pattern recognition using a three-dimensional accelerometer and support vector machines," *Applied Animal Behaviour Science,* vol. 119, no. 1, pp. 32-38, June 2009, doi: https://doi.org/10.1016/j.applanim.2009.03.005.

[31] J. A. Vázquez Diosdado *et al.*, "Classification of behaviour in housed dairy cows using an accelerometer-based activity monitoring system," *Animal Biotelemetry,* vol. 3, no. 1, June 10 2015, doi: 10.1186/s40317-015-0045-8.

[32] R. Arablouei, L. Currie, B. Kusy, A. Ingham, P. L. Greenwood, and G. Bishop-Hurley, "In-situ classification of cattle behavior using accelerometry data," *Computers and Electronics in Agriculture,* vol. 183, p. 106045, April 2021, doi: 10.1016/j.compag.2021.106045.